

CLIC DRIVE BEAM FREQUENCY MULTIPLICATION SYSTEM DESIGN

C. Biscari, D. Alesini, A. Ghigo, F. Marcellini, LNF-INFN, Frascati, Italy
 B. Jeanneret, CERN, Geneva, Switzerland

Abstract

The CLIC drive beam current, produced by the 1 GHz fully loaded Linac, will be multiplied by a factor of 24 by the frequency multiplication system, to generate the high power beam representing the CLIC power source. The frequency multiplication system is composed by one Delay Loop plus two Combiner Rings. All rings will be isochronous, will contain trajectory tuning wigglers, and all magnets will be normal conducting. The design of the rings, with special emphasis on the rf deflectors characteristics, is presented.

INTRODUCTION

The power for feeding the 12 GHz Main Linacs of the CLIC collider is extracted from the high current drive beam. The drive beam is accelerated to 2.37 GeV by a normal conducting 1 GHz Linac, after which a frequency multiplication system (fms) compresses the beam pulses up to an average current over the pulse of 100 A. The compression is obtained by recombining the bunches in successive rings and using rf deflectors. The system is designed to preserve transverse and longitudinal beam emittances: isochronicity, smooth linear optics, low impedance vacuum chambers and diagnostics, HOM free rf active elements, are foreseen. In CTF3[1] the recombination feasibility in the Combiner Ring has been demonstrated for a low energy beam (120 MeV), up to 12A (140 nsec). The design of CLIC fms is essentially based on the CTF3 design and results. CLIC drive beam main parameters are summarized in Table 1, compared to those of CTF3.

Three recombination stages are foreseen: a Delay Loop (DL) for the first factor of 2, a first Combiner Ring (CR1) for a factor of 3, and a second one (CR2) for the last factor of 4. The layout of the whole fms is shown in Figure 1. The two smaller rings are housed inside CR2 to optimise space requirements.

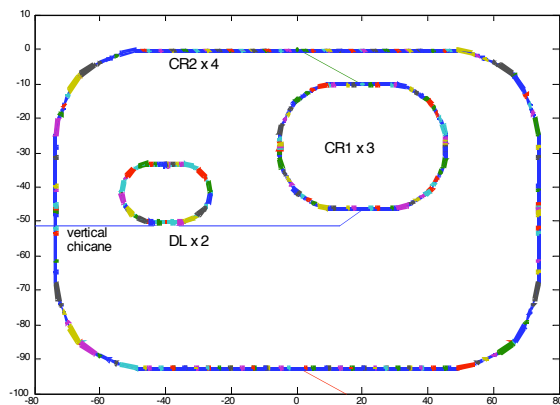


Figure 1: Layout of the CLIC frequency multiplication system.

A vertical chicane is used in the injection transfer line, and it can act as a bunch stretcher, as in the CTF3 system. It is useful to adjust the bunch length in order to minimize coherent synchrotron radiation effects on bunch length and energy spread.

Table 1: CLIC drive beam main parameters after the recombination compared to CTF3 ones

Parameter	CTF3	CLIC
Energy, $E_{in,dec}$, GeV	0.150	2.37
Pulse average current, I_{dec} , A	35	100
Train duration, τ_{train} , ns	140	244
No. Bunches / train, N_b	1600	2922
Bunch charge, Q_b , nC	3	8.4
Bunch separation, Δ_b , ns	0.083	0.083
Rms bunch length, σ_s , mm	1	1
Rms emittance, $\gamma\epsilon$, $\mu\text{m rad}$	100	150

ISOCHRONOUS RINGS

The length of the three isochronous rings is determined by the temporal structure of the drive beam. The DL will have the length of the final bunch train (244 nsec or 73 m), while CR1 and CR2 lengths will be its multiples ($L_{CR1} = 2L_{DL}$, $L_{CR2} = 3L_{CR1}$). Their main parameters are listed in Table 2. To be noticed that the bunch length is longer than the final one (Table 1), since the bunches will be stretched before entering in the fms and then compressed before the deceleration, to mitigate collective effects driven by high peak currents.

All the magnets are based on normal conducting technology. The optics design allows a large range of tunability in transverse phase advances, essential for optimising the system operation, as shown in CTF3.

Table 2: CLIC fms main parameters

Parameter	DL	CR1	CR2
Emittance [$\mu\text{m rad}$]	< 100	< 100	< 100
Energy spread	< 1 %	< 1 %	< 1 %
Bunch length [mm]	2	2	2
L [m]	73	146	438
Combination factor	2	3	4
RF deflector fr [GHz]	1.5	2.	3.
N of dipoles	12	12	16
Dipole ρ [m]	4.7	4.7	12.0
N of quads / families	18 / 9	48 / 9	64 + fodo
I_q dB/dx max [T]	10.2	5.1	3.2
N of sexts / families	6 / 3	24 / 3	24/3
I_s d^2B/dx^2 max [Tm^{-1}]	22	40	48

Delay Loop, DL

The DL is a single pass line. The dipoles occupy a large part of it, and they have a weak field index, which helps in minimizing the quadrupoles number. The isochronicity condition is satisfied on half the ring. A trajectory tuning wiggler is placed at the midpoint of the line. The rf deflector at 1.5 GHz kicks the beam of a 5 mrad angle. In order to relax the septum parameters, a defocusing quadrupole is in between the deflector and the septum. It acts on both the incoming and the outgoing beams thus increasing their relative separation at the septum location.

First Combiner Ring, CR1

The CR1 design is very similar to the CTF3 CR one: four isochronous arcs, two long straights for injection and extraction and two short ones housing the trajectory length tuning wigglers. Each arc has three dipoles, and two symmetric quad triplets. Two rf deflectors at ~ 2 GHz, placed at π horizontal phase advance, are used for the bunch train injection and recombination.

2nd Order Chromatic Effects

The high order terms of transverse and longitudinal chromaticity must be corrected simultaneously in order to ensure preservation of beam emittances in all the planes. The final correction must take into account the whole fms. At this design stage the correction in CR1 is being faced, and the rest of the system will be later integrated.

In CR1 it is quite easy to satisfy the isochronicity condition at 2nd order by matching $T_{566} = 0$ with a single family of sextupoles, 2 elements per arc (the other contributing terms $T_{511}D_x^2(s=0) \dots$ etc, are all negligible). Correcting in addition the chromaticity and limiting 2nd order aberrations for large momentum spread is more complex. At the sextupole location the dispersion is large ($D = 1.5$ m), and the ratio $\beta_y/\beta_x = 0.4$ is small (see Fig. 2).

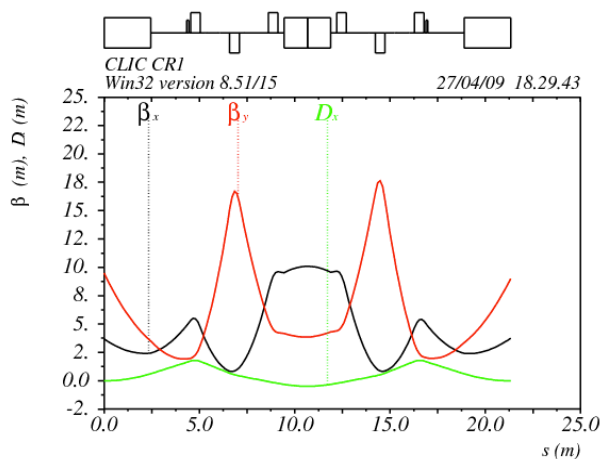


Figure 2: Optical functions in CR1 arc.

The horizontal phase advance between the two sextupoles is very close to a multiple of $\pi/2$, nicely limiting the chromatic β -beating in this plane. In the vertical plane the small β_y helps to limit the beating, so that the maximum beating along the ring is small in both

planes ($\Delta\beta/\beta < 0.22$ for 2% of δp). The horizontal chromaticity is corrected to an acceptable level ($Q'_x = -9.8$ sext off, and -2.1 sext on), and the vertical one increases slightly ($Q'_y = -10.4$ sext off, and -13.6 sext on). The phase error per turn in the horizontal plane is small, while it is not negligible in the vertical plane for which a second family of sextupoles may be necessary.

The present work was made using the PTC code [2][3], which is now implemented inside madX. Comparisons with analytical calculations made with simple systems show that PTC is perfectly accurate whatever the momentum offset.

An exhaustive view of the degradation of the phase-space is obtained by tracking particles of betatronic amplitudes $A_{x,y} = 1,2,3 \sigma_{x,y}$ evenly spaced in phase and covering the momentum range $\pm 2\%$ over three turns.

For each of the four transverse coordinates, the following quantities are built, with the index x standing for each of the four canonical variables x, px, y, py

$$\begin{aligned} h_{x+}(\delta_p) &= [x_{\max}(\delta_p) - x_{\text{av}}(\delta_p)] \sigma_{\beta,x} \\ h_{x-}(\delta_p) &= [x_{\text{av}}(\delta_p) - x_{\min}(\delta_p)] \sigma_{\beta,x} \\ h_{x0}(\delta_p) &= x_{\text{av}}(\delta_p) \sigma_{\beta,x} \end{aligned} \quad (1)$$

Plots on the right in Fig. 3 indicate no significant deformation of the vertical phase-space. On the other hand, the horizontal phase-space is preserved up to $\delta p = \pm 1.2\%$. Near $\delta p = \pm 2\%$, the beam-centroid is moved by $0.7\sigma_x$ due to the presence of a residual chromatic dispersion. The ct distribution is adequately good. The peak error $\delta ct = 0.5$ mm at $\delta p = -2\%$ must be compared to a rms bunch length of 2 mm.

It remains to explore the whole fms with a more detailed tracking where 6D-gaussian distributions will be used.

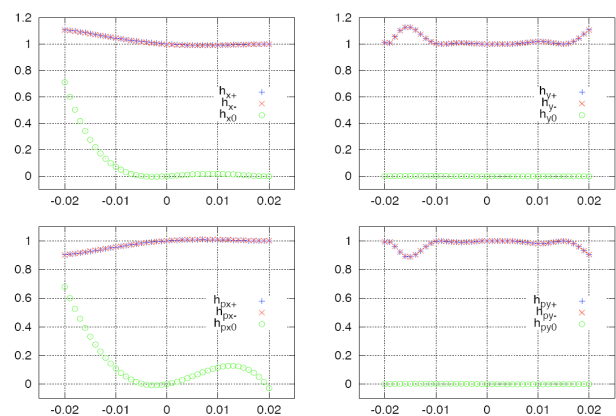


Figure 3: Functions $h(\delta_p)$ for the 4 canonical transverse phase space variables.

Second Combiner Ring, CR2

The energy lost by synchrotron radiation emission per turn is $U_0(\text{MeV}) = 2.8/\rho(\text{m})$ for the nominal beam energy, where ρ is the dipole bending radius. CR2 is the ring where the bunches travel longer, and it is also the one

where more space is available, so a longer bending radius has been chosen, in order to minimize the energy spread among bunches following different recombination arcs. The optical structure is similar to CR1 one, with the difference that each isochronous arc has four dipoles, with a quadrupole in between the two central ones. FODO sections fill the ring up to the necessary length. Figure 4 shows the optical functions in the isochronous arc.

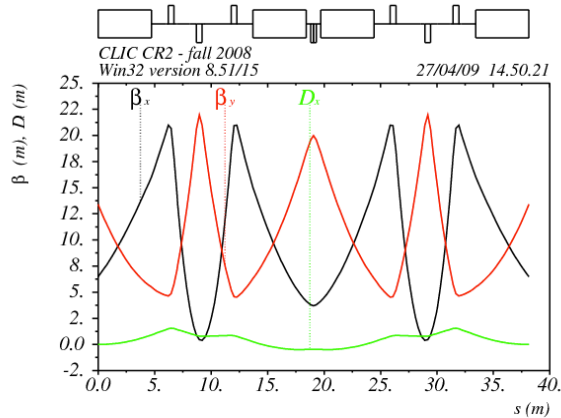


Figure 4: Optical functions in CR2 arc.

INJECTION AND EXTRACTION

The beam injection and extraction in and from the three rings is done through CW septa magnets placed in the straight sections. The lattices of these sections have been designed to reduce the requested deflection angle. Magnets similar to the CTF3 septa can be used, in spite of the higher energy, giving to the CLIC drive beam a deflection angle of 25 mrad, with a septum thickness of 12 mm, a magnetic length of 650 mm and a current of 2000A. A longer magnet, with less stringent parameters, follows this septa and guides the beam into the nominal trajectory.

Several RF deflector options for the three systems have been considered. The frequency of each deflector can be chosen as the minimum dictated by the bunch frequency and recombination factor or as one of its multiples. Respectively 1.5, 2 and 3 GHz have been chosen for the DL, CR1 and CR2.

Both standing wave (SW) and travelling wave (TW) structures can in principle be used, and they both have been analyzed. The main results, obtained by scaling the parameters of the existing CTF3 RF deflectors [4, 5], are reported in Tables 3 and 4. For SW deflectors, an input coupling coefficient equal to 1 (to avoid reflected power from the cavity to the klystron and maximize the deflecting efficiency) and π -mode-like multi-cell structures have been considered. On the other side $2\pi/3$ mode has been chosen in the case of TW structures.

Using SW structures the number of cells and the necessary RF input power can be reduced with respect to the TW option. Nevertheless, the average dissipated power per cell is higher and the cooling system can be difficult to realize. The average dissipated power results

so high because of the very long pulse ($\sim 140 \mu\text{s}$) and high repetition rate (50 Hz) of the CLIC linac pulse. Since the linac pulse is much longer if compared with the typical SW cavities filling time, it is not necessary to overcouple the SW cavities as done for the CTF3 delay loop [5].

The interaction between the RFD and the trains of bunches is being evaluated by means of beam loading calculations, as done in the CTF3 case [5, 6].

Solutions to damp possible HOMs and deflecting modes with tilted polarity will be implemented, as done in the upgraded CTF3 CR deflector [7], to avoid possible induced beam instabilities.

Table 3: RF deflectors SW option (b=cell radius, L=total length, τ_f =filling time, P_{in} =input power, P_d =average single cell dissipated power, N=number of cells)

Ring	f [GHz]	N	b [mm]	L [m]	τ_f [μs]	P_{in} [MW]	P_d [kW]
DL	1.5	8	122	0.4	3.1	11	10
CR1	2	8	91	0.3	2	12	11
CR2	3	12	61	0.3	1.1	10	12

Table 4: RF deflectors TW option (a=iris radius)

Ring	f [GHz]	N	a [mm]	L [m]	τ_f [μs]	P_{in} [MW]	P_d [kW]
DL	1.5	18	28	1.2	0.25	50	3
CR1	2	18	21	0.9	0.2	50	3.3
CR2	3	27	23	0.9	0.14	20	3

CONCLUSIONS

The main elements of the CLIC drive beam frequency multiplication system have been defined, basing most of the design considerations on CTF3 results. The magnetic and optical layout of the three isochronous rings needed for the recombination have been studied. High order chromaticity correction in transverse and longitudinal planes is in progress.

It has been shown that the choice of rf deflector frequency can be flexible and both TW and SW structures can be chosen for the three ring.

The septa design, which is one of the most challenging devices of the system, has been addressed.

REFERENCES

- [1] S. Bettoni et al., FR1RAC04, this conference.
- [2] Introduction to the Polymorphic Tracking Code, E. Forest, F. Schmidt and E. McIntosh, KEK Report 2002-3, July 2002, A/M.
- [3] The madX home page. <http://frs.web.cern.ch/frs/Xdoc/mad-X.html>
- [4] D. Alesini, et al., EPAC 2002, p. 2115.
- [5] D. Alesini and F. Marcellini, PRST AB 12, 0313301, (2009).
- [6] D. Alesini and A. Gallo, PRST AB 7, 034403, (2004).
- [7] D. Alesini, et al., WE1PBC04, this conference.